MRS Communications (2025) 15:1323–1330

https://doi.org/10.1557/s43579-025-00799-6

MRS Communications

Early Career Distinguished Presenter Research Letter

Enhancing wet adhesion in biodegradable hydrogels via water-absorbent integration

Jing Er Tan, and Shengnan Liu, School of Materials Science and Engineering, Tsinghua University, Beijing 100084, People's Republic of China
Jun Bai, Department of Neurosurgery, Xuanwu Hospital, Capital Medical University, Beijing 100053, People's Republic of China
Bingbing Yu, and Kuntao Chen, School of Materials Science and Engineering, Tsinghua University, Beijing 100084, People's Republic of China
Xing Sheng, Department of Electronic Engineering, Tsinghua University, Beijing 100084, People's Republic of China; IDG/McGovern Institute for Brain Research, Tsinghua University, Beijing 100084, People's Republic of China; State Key Laboratory of Flexible Electronics Technology, Beijing 100084, People's Republic of China; Institute for Precision Medicine, Tsinghua University, Beijing 100084, People's Republic of China; Beijing National Research Center for Information Science and Technology, Tsinghua University, Beijing 100084, People's Republic of China
Lan Yin, School of Materials Science and Engineering, Tsinghua University, Beijing 100084, People's Republic of China; State Key Laboratory of Flexible Electronics Technology, Beijing 100084, People's Republic of China; The Key Laboratory of Advanced Materials of Ministry of Education, Tsinghua University, Beijing 100084, People's Republic of China

Address all correspondence to Xing Sheng at **xingsheng@tsinghua.edu.cn**

(Received 17 June 2025; accepted 8 August 2025; published online: 25 August 2025)

Abstract

Wet-adhesive hydrogels hold significant promise for biomedical applications, yet achieving long-term adhesion remains a major challenge in biodegradable systems. Here, we present a biodegradable hydrogel incorporating a water-absorbent layer to regulate swelling behavior and water content. Comprising a poly(ethylene glycol) diacrylate (PEGDA)–gelatin matrix with a starch-based absorbent layer, the hydrogel exhibits high wet adhesion energy, elevated burst pressure, effective *in vivo* hemostasis, and mechanical compatibility with soft tissue. This water-absorbent strategy provides a new avenue for achieving sustained and stable wet tissue adhesion in biodegradable hydrogel systems.

Introduction

Adhesive hydrogels combine biocompatibility, mechanical compliance, and tissue adhesion in wet physiological environments, supporting essential biomedical applications such as hemostasis,[1–6] anastomosis,[7–10] and the stabilization of bioelectronic interfaces.[11–15] Through the rational design of interfacial bonding chemistries[10,11,16] and network architectures,[9,17–19] a variety of hydrogel-based tissue adhesives have demonstrated promising capabilities, including high tissue adhesion strength,[17,20] robust mechanical properties,[16,19] and efficient drug delivery.[4,21] A key challenge, however, lies in maintaining strong and stable adhesion in wet and dynamic physiological environments over prolonged periods. Continuous blood flow and interfacial liquids can impede the formation of robust adhesive interactions. In addition, hydrogel swelling and excessive water content dilute the density of reactive functional groups and weaken the crosslinked network, thereby compromising both adhesive strength and mechanical integrity over time.[2] Swelling-induced compression of surrounding tissues may also lead to secondary damage.[3] To address these issues, several strategies have been developed, including repelling or absorbing interfacial hydration layers,[22] using controlled porosity to modulate water penetration,[5] and applying pre-stretching to limit swelling upon water absorption.[23] Nevertheless, despite significant advances, developing wet adhesive hydrogels that combine long-term adhesion with biodegradability remains a challenge. The presence of non-degradable or proinflammatory components to promote adhesion may necessitate secondary surgical removal and is associated with elevated risks of infection and tissue damage.

In this study, we developed a biodegradable hydrogel composed of a poly(ethylene glycol) diacrylate (PEGDA)–gelatin matrix (PG hydrogel), with an upper surface layer of starch serving as a water absorbent, referred to as the PG-S hydrogel. This design effectively modulates swelling behavior and water content over time, leading to enhanced long-term tissue adhesion and increased burst pressure. *In vivo* studies in rodents demonstrate rapid and effective hemostasis with the PG-S hydrogel. This work highlights a materials strategy for the development of biodegradable hydrogels with robust wet tissue adhesion and extended stability under dynamic, aqueous physiological conditions.

Materials and methods

The synthesis of PG-S hydrogel

The PG-S hydrogel is based on our previously reported PG hydrogel design,[24] with the incorporation of a water-absorbent layer. Briefly, 20 wt% PEGDA (20,000 Da, Yare), 5 wt% gelatin (Aladdin), 1.2 wt% sulfo-NHS (Meryer), and 0.036 wt% photoinitiator Irgacure 2959 (I-2959, Meryer) were dissolved

Jing Er Tan and Shengnan Liu contributed equally to this work.

in deionized water and stirred at 60°C for 4 h. Genipin (Meryer) was then added to form the precursor solution. After degassing, the solution was cast into a Teflon mold and cured under UV light (365 nm, 8 mW cm^{-2}) for 20 min. A water-absorbent layer was formed by applying starch (Xianding) at 0.05 g cm^{-2} to the upper surface of the crosslinked hydrogel through sieving. The PG-S hydrogel was then pre-stretched along the x–y direction and air-dried overnight at room temperature to further constrain the swelling. For adhesion, a bridging agent consisting of 2 wt% chitosan (190,000–310,000 Da, Sigma-Aldrich) and 1 wt% genipin in MES buffer was applied to the surface prior to bonding. The control PG hydrogel was prepared using the same protocol without starch loading.

Materials characterization

Microstructure and degradation properties

Scanning electron microscopy (SEM, Merlin, Zeiss) was employed to characterize the surface and internal morphology of the hydrogel. Samples were freeze-dried and sputter-coated with platinum prior to imaging. Cross-sectional morphology was revealed by fracturing the hydrogel in liquid nitrogen.

In vitro *degradation behavior*

Hydrogel degradation was evaluated *via* accelerated degradation testing in phosphate-buffered saline (PBS). Dried hydrogel samples were weighed (W_0) and immersed in PBS at 65°C. Photographs were taken at different stages. Samples were removed at different time points, thoroughly rinsed, dried, and reweighed (W_t). The remaining mass percentage was calculated as $(W_0 - W_t)/W_0 \times 100\%$.

Water content and swelling ratio

To measure the water content, dried hydrogels were weight (W_D) and soaked in PBS at 37°C. At different time points, hydrogels were taken out and remove surface water. The wet mass W_S was measured. Water content was calculated as $(W_s - W_D)/W_s \times 100\%$. Swelling ratio was calculated as $(W_s - W_D)/W_D \times 100\%$.

Mechanical properties and adhesion energy

Dried hydrogels were cut into dumbbell shapes (ISO 527-3 5B, $L_0 = 10$ mm, $b = 2$ mm, $h = 1$ mm). The stress–strain curves were measured using a universal testing machine (EZ-LX HS, Shimadzu) at a constant stretching speed of 20 mm/min. The corresponding breaking stress, elongation at break, and Young's modulus were calculated. Lap shear test and 180° peel test were performed to evaluate the adhesion properties of hydrogel. Muscle tissues from sacrificed New Zealand white rabbit were cut into the same shape as the hydrogel, rinsed with PBS, and treated with the bridging agent. After adhering dried hydrogel to the tissue, the sample was soaked in PBS at 37°C. Samples were collected at different time points to measure the hydrogel's water content and to perform adhesion energy tests. The adhesion tests were performed using universal testing machine (EZ-LX HS, Shimadzu) at a constant stretching speed of 5 mm/min. Adhesion energy was calculated from the plateau force ($F_{plateau}$) in 180° peel test and width of the hydrogel sample, $2F_{plateau}/w$. Lap shear strength was calculated from the maximum force and adhesion surface area, $F_{max}/(w \times L)$.

Liquid burst pressure test

A perforated ovine aorta tissue was fixed onto the device chamber, with the hydrogel applied at the perforation site. The chamber was then inverted and immersed in PBS to fully soak the hydrogel and tissue, simulating an *in vivo* wet environment. PBS was pumped through the chamber to the adhesion interface at different time points, and the pressure was recorded using a pressure gauge. The maximum pressure at which adhesion failure or hydrogel rupture occurred was recorded as the burst pressure.

In vivo *hemostasis performance in liver rupture model*

A 3-mm penetrating puncture wound was created at the edge of the left liver lobe of Sprague–Dawley (SD) rats. The rupture was immediately treated with either PG-S hydrogel or a commercial tissue adhesive (508 Glue, Butyl cyanoacrylate, COMPONT) applied to both sides of the wound. The time to hemostasis was recorded, and blood loss during the procedure was absorbed using gauze. The change in gauze weight was measured to quantify the amount of blood loss. Experiments involving animals were conducted in accordance with the protocols approved by Experimental Animal Ethics Committee of Tsinghua University (18-SX1.G22-1).

Results and discussion

Material strategies for biodegradable adhesive hydrogels to promote stable wet adhesion

Controlling the water content and swelling ratio of adhesive hydrogels is essential to facilitate long-term stable adhesion to tissues in physiological environments. Building on our previously reported biodegradable adhesive PG hydrogel,[24] we introduce a strategy that integrates a water-absorbent layer onto the top surface of the hydrogel matrix to regulate swelling, resulting in the PG-S hydrogel. Starch is selected as the absorbent due to its inherent biodegradability and biocompatibility. A schematic illustration of the PG-S hydrogel is shown in Fig. 1(a). Starch is applied to the upper surface of a dried, pre-stretched PG hydrogel matrix, while the opposite surface interacts with tissue. The starch particles were loaded to the hydrogel surface to saturation, such that no further adhesion of starch was observed, and no exposed hydrogel surface remained, thereby maximizing the water absorbing effect of the starch layer. The interaction between

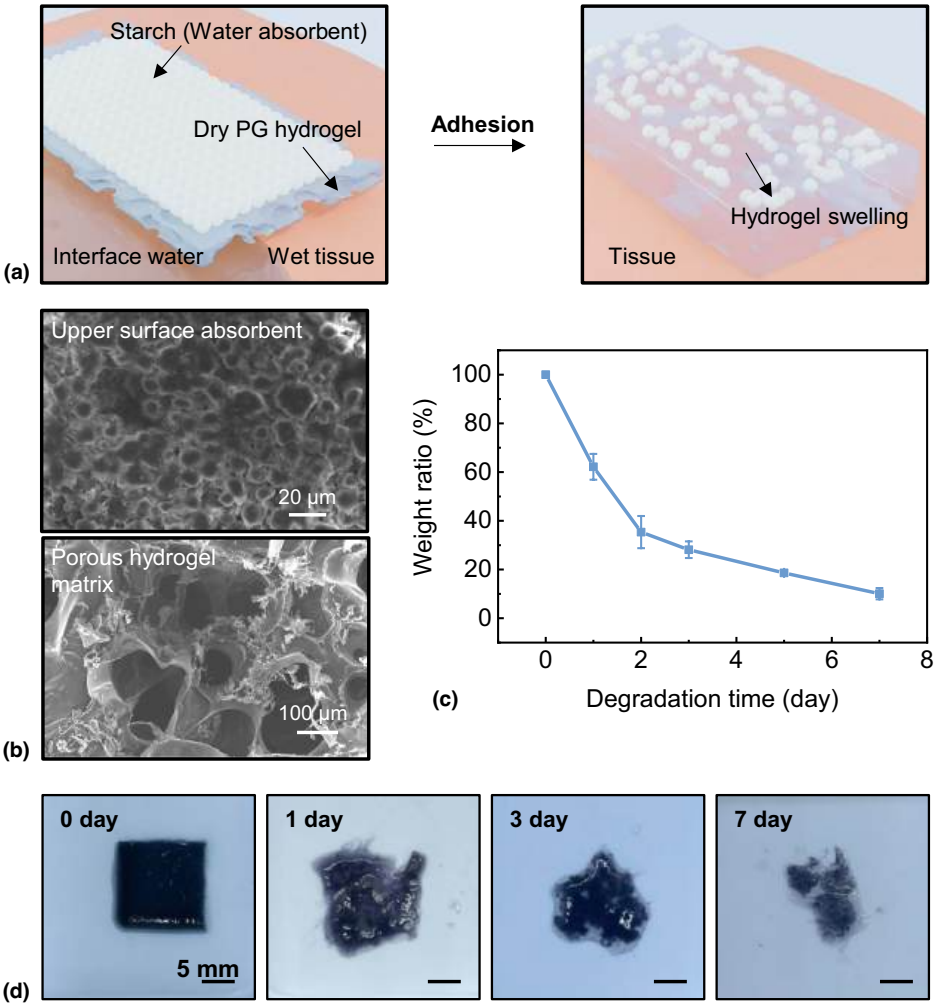

Figure 1. Mechanism of enhanced adhesion in hydrogel *via* water absorbents and degradation profile. (a) Schematic diagram of the absorption of interfacial water by the dried hydrogel loaded with water absorbents, extending the duration of robust wet adhesion. (b) Scanning electron microscopy (SEM) image of the upper surface with water absorbents and the cross section of hydrogel. (c) Weight ratio of hydrogel during degradation process in 65°C PBS. (d) Photographs of hydrogel during degradation process in 65°C PBS. In (c) all data are presented as mean ± standard deviation. $n = 5$ independent experiments.

starch particles and the PG hydrogel matrix is driven by multiple interaction including hydrogen bonds,[25] van der Waals forces, and capillary forces,[26] due to the presence of hydroxyl groups in starch and the rich functional groups in PG hydrogel. The large effective surface area of the starch particles, together with the soft hydrogel surface, facilitates extensive contact and firm adhesion between the two layers, laying a solid foundation for its effective application. Pre-stretching the dried hydrogel can facilitate constraining swelling, as previously reported.[23] Upon contact, interfacial water is rapidly absorbed through the hydrogel matrix and by the starch layer, promoting timely formation of both physical and covalent bonds at the tissue interface at the initial stage. The starch layer helps modulate water content and limits hydrogel swelling over time, thereby sustaining stable adhesion. Additionally, this top layer provides a non-adhesive surface, enabling convenient handling while minimizing unintended adhesion to surrounding tissues.

SEM images in Fig. 1(b) reveal that the upper surface of the hydrogel is coated with starch particles, forming a rough, textured morphology. No exposed hydrogel surface can be observed, indicating that the starch particle loading reached saturation and that the particles adhered firmly to the PG hydrogel surface. The cross section of the dried hydrogel matrix exhibits a porous structure. To assess the biodegradability of the PG-S hydrogel, accelerated degradation tests are conducted in PBS at an elevated temperature of 65°C. Changes in morphology and the residual mass ratio are monitored over time [Fig. 1(c), (d)]. The hydrogel exhibits rapid weight loss within the first two days, after which the degradation rate slows down [Fig. 1(c)]. Approximately 35% of the initial mass remains at day 2, decreasing to 18% by day 5 and 10% by day

7. Morphological changes over time are shown in Fig. 1(d). The hydrogel exhibits a blue color, attributed to the presence of genipin in the composition.[27] After one day, visible fragmentation occurs while the overall volume is largely retained. By day 3, the hydrogel exhibits substantial volume shrinkage and disintegrates into smaller fragments. At day 7, the structure had almost completely broken down into flocculent debris. As starch is a naturally derived and biodegradable material, its incorporation as a water absorbent does not compromise the hydrogel's degradability. These results indicate that the PG-S hydrogel can degrade in aqueous environments, therefore eliminating the need for surgical removal and avoiding unnecessary material retention. Compared with the previously reported similar structured hydrogel that retained over 50% of its mass after ~30 days at 37°C,[24] PG-S hydrogel is expected to exhibit comparable or even slower degradation under physiological conditions. This degradation behavior ensures that it maintains functional integrity during the intended working period and subsequently undergoes degradation.

The effect of starch on mechanical, swelling, and adhesion properties of PG-S hydrogels

Given that hydrogel adhesion performance is highly dependent on water content,[28] as lower water content leads to shrinkage in hydrogel volume, results in higher surface chain density to form adhesion with tissue surface. We first evaluate adhesion energy and shear strength of hydrogel with rabbit muscle tissue as a function of water contents using 180° peel and lap shear tests, after 1 h of contact in aqueous conditions. Water content is controlled by soaking dried hydrogels in PBS for predetermined durations followed by weighing. Bridging agents containing chitosan and genipin are applied at the interface to assist adhesion. The results show that both adhesion energy and lap shear stress demonstrate a lower value with hydrogel

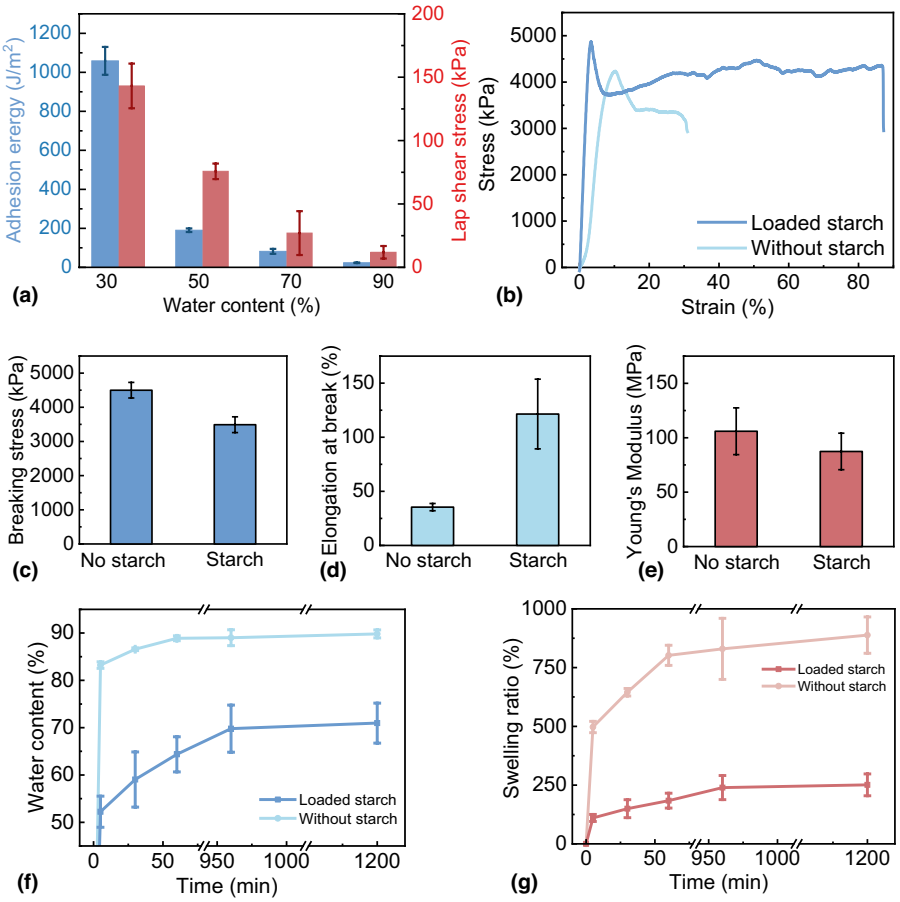

Figure 2. Effects of starch water absorbents on the mechanical properties, water content, and swelling ratio of hydrogels. (a) Adhesion energy and lap shear stress of hydrogels with different water contents. (b) Stress–strain curve of hydrogel with or without starch loading. The (c) breaking stress, (d) elongation at break, and (e) Young's modulus derived from stress–strain curve of hydrogel with or without starch. The (f) water content and (g) swelling ratio of hydrogel with or without starch. All data are presented as mean ± standard deviation. In (a)–(g), $n = 5$ independent experiments.

of higher initial water content [Fig. 2(a)]. For hydrogel with 70% water content, the adhesion energy is 3.6 times greater than that of hydrogel with 90% water content. These results suggest that controlling water content and swelling can promote interfacial adhesion.

We then assess the mechanical performance of PG-S hydrogels by comparing the stress–strain profiles of dried hydrogels with and without the starch layer [Fig. 2(b)]. The results show that the tensile strength decreases slightly upon starch loading [Fig. 2(c)], while the elongation at break increases markedly from 35.4 ± 3.3 to 121.4 ± 32.2% [Fig. 2(d)]. This may be attributed to energy dissipation at the hydrogel–starch interface. The interactions between starch particles and the hydrogel such as hydrogen bonds serve as "sacrificial bonds,"[29] as the energy accumulated under external force tends to be released through the breaking of these weaker interactions.[30,31] Such energy dissipation can mitigate damage to crosslinking in the hydrogel network, thereby enhancing the elongation capacity. Moreover, the Young's modulus decreases slightly with the addition of starch [Fig. 2(e)]. Overall, the starch layer imparts enhanced flexibility and stretchability to the dried hydrogel, while only slightly compromising tensile strength.

To investigate the influence of starch on swelling, we quantify water content and swelling ratios of PG and PG-S hydrogels incubated in PBS over time. As shown in Fig. 2(f), the PG-S hydrogel exhibits reduced water uptake, reaching a swelling equilibrium at a water content of ~ 70%, compared to ~ 90% in the starch-free hydrogel. Notably, the initial water uptake is also slower in PG-S hydrogels, with the PG hydrogel exceeding 80% water content within 5 min, whereas the PG-S hydrogel demonstrates a moderated increase, indicating that starch efficiently absorbs water at the early stage and regulates subsequent swelling. The reduced water content also leads to a significant decrease in swelling ratio. After 1200 min in PBS, the swelling ratio of PG-S hydrogels is 251 ± 47%, compared to 888 ± 77% for the PG hydrogel [Fig. 2(g)]. The constrained water uptake (~ 70%) allows maintaining crosslink density and surface functional group availability, factors that contribute to sustained adhesion strength and prolonged mechanical stability.[28] Additionally, reduced swelling mitigates the risk of hydrogel-induced compression on surrounding tissues. Although hydrogels with lower water content may further enhance adhesion energy, they often exhibit mechanical moduli that are incompatible with soft tissues. A water content of approximately 70% is therefore considered optimal, offering a balance between mechanical strength, tissue conformity, and adhesive performance.[28]

The adhesion of PG-S hydrogels with rabbit muscle tissue over time in aqueous environments is measured using a lap shear test. Specifically, the dried PG-S hydrogel is brought into contact with the tissue and soaked in PBS at 37°C, and the adhesion energy is assessed at different time points. The results show that adhesion energy increases rapidly after 15 min [Fig. 3(a)] due to the continuous formation of strong covalent bonds between PG-S hydrogel and the tissue surface. The addition of starch enhances adhesion energy from 415 ± 69 to 718 ± 143 J/m^2 after 30 min of adhesion. This suggests that the water-absorbent layer promotes adhesion at the initial stage by removing interfacial water, creating favorable conditions for the formation of strong covalent bonds. After 60 min of adhesion, PG-S hydrogel shows a high adhesion energy of 1829 ± 73 J/m^2, compared to 1422 ± 275 J/m^2 for hydrogel without starch [Fig. 3(b)], likely due to its lower swelling ratio.

Furthermore, long-term adhesion between PG-S hydrogel and tissue is evaluated for several days. As shown in Fig. 3(c), during the first four days, the effect of starch as a water absorbent remains significant. On day 4, PG-S hydrogel maintains a moderately high adhesion energy of 97 ± 17 J/m^2, while hydrogel without starch exhibits a much lower adhesion energy of 63 ± 10 J/m^2. This difference is mainly attributed to starch's inhibition of swelling. After day 5, the adhesion energies of the PG-S and PG hydrogels become similar and gradually decrease over time, likely because the water absorbent becomes less effectively regulate swelling. These results suggest that the incorporation of starch enhances sustained tissue adhesion for several days, until saturation occurs.

The burst pressure tolerance of PG-S hydrogel is also assessed using the setup illustrated in Fig. 3(d). The hydrogel is adhered to a perforated ovine aorta tissue and soaked in PBS. The maximum liquid burst pressure that the hydrogel–tissue interface can withstand is measured by injecting PBS into the perforation at various time points. At the initial stage, the burst pressure increases gradually with adhesion time and exhibits a significant rise after 15 min as the covalent bonds begin to form. The highest burst pressure recorded for PG-S hydrogel is 318 ± 12 mmHg after 3 h of adhesion, which decreases to around 200 mmHg after 24 h and remains stable for at least 21 days [Fig. 3(e)]. These results demonstrate the long-term stability of PG-S hydrogel adhesion in aqueous conditions. Moreover, the burst pressure tolerance exceeds typical clinical values, such as systolic blood pressure (~ 120 mmHg). The rapid increase in burst pressure during the initial stages further highlights the potential of PG-S hydrogel for timely wound closure or anastomosis.

Hemostasis performance of PG-S hydrogel

To evaluate the *in vivo* wet adhesion strength and hemostatic performance of the PG-S hydrogel, a liver rupture model in SD rats is used. Liver perforations are treated with either PG-S hydrogel or a commercial 508 tissue adhesive as a control. The surgical setup and bleeding conditions are shown in Fig. 4(a). The perforations treated with PG-S hydrogel stop bleeding within 26 s, while bleeding in the commercial adhesive group persists beyond 150 s. Additionally, the starch layer on the hydrogel's surface prevented unwanted adhesion to surrounding tissues, minimizing secondary damage. In contrast, the commercial adhesive causes undesired adhesion to adjacent tissues, as shown in Fig. 4(a). The hardened, warped edges of the commercial adhesive indicate poor mechanical compatibility and instability in soft tissue environments.

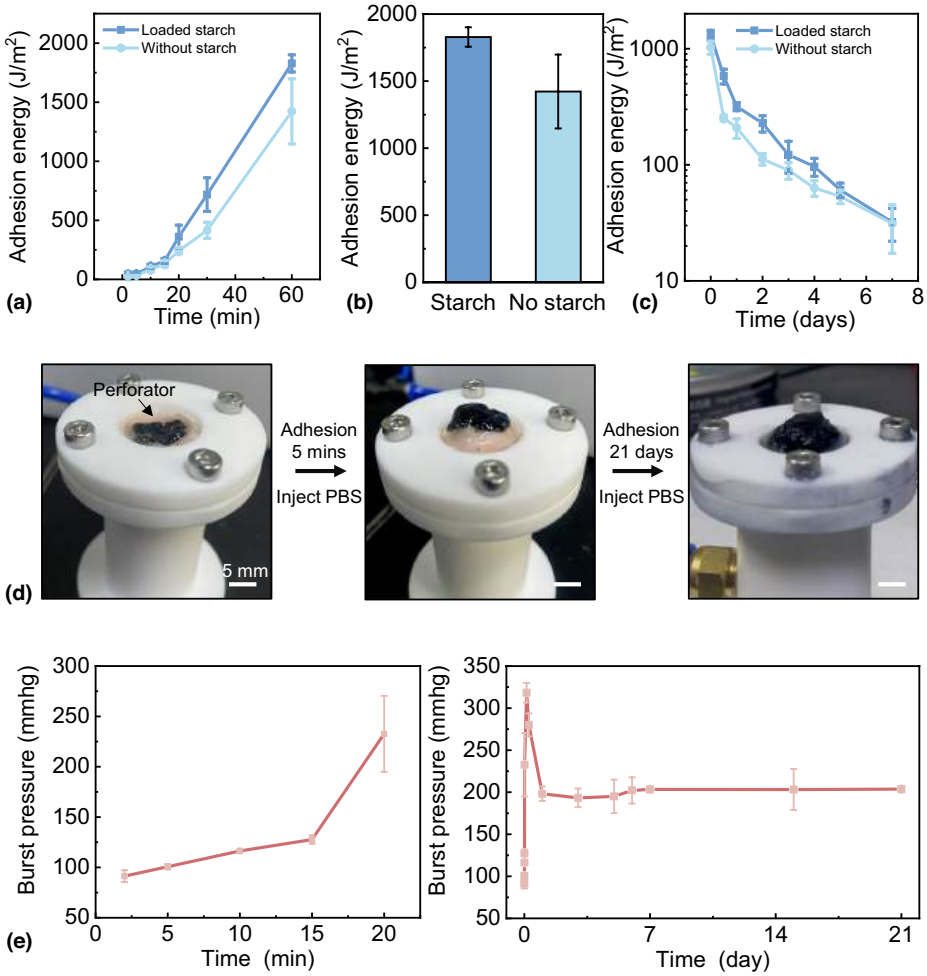

Figure 3. Water absorbents improve the wet adhesion performance of hydrogels. (a) The effect of starch on the rapid formation of adhesion between the hydrogel and the muscle tissue of rabbits. (b) The difference in adhesion energy of hydrogel with or without starch measured at 1 h. (c) The effect of starch on the long-term stable adhesion between the hydrogel and rabbit muscle tissue. (d) The photographs of the burst pressure measurement of the hydrogel after adhesion to the ovine aorta tissue at different stages. (e) The burst pressure measured using PBS injection of PG-S hydrogel adhered to the ovine aorta tissue as a function of time. All data are presented as mean ± standard deviation. In (a)–(c) $n = 5$ independent experiments. In (e) $n = 3$ independent experiments.

PG-S hydrogel maintains robust adhesion to the liver tissue, with the interface remaining stable under pulling force after 5 min of adhesion [Fig. 4(b)]. Total blood loss during the procedure is summarized in Fig. 4(c). The commercial adhesive group lost 1.31 ± 0.37 g of blood, whereas the PG-S hydrogel group shows significantly less blood loss, at 0.54 ± 0.10 g. These results demonstrate desirable hemostatic performance, dynamic tissue adaptability, and reliable wound closure capability of PG-S hydrogel compared to conventional 508 adhesives.

Conclusion

In summary, we demonstrate the morphology, mechanical properties, wet adhesion performance, and *in vivo* hemostatic capability of a biodegradable, starch-loaded PG-S hydrogel as an effective strategy to enhance prolonged wet adhesion. With a control of water content and swelling ratio, the PG-S hydrogel achieves excellent wet adhesion energy of 1829 ± 73 J/m^2 and a high burst pressure of 318 ± 12 mmHg at short term, and allows robust long-term adhesion with a burst pressure of around 200 mmHg at day 21. The biodegradability eliminates retrieval surgical process and therefore significantly reduces potential infection risks. *In vivo* hemostasis tests in rodents demonstrate rapid bleeding control, highlighting the superior performance of the hydrogel compared to commercial 508 adhesives. This strategy offers a promising approach to modulate water content and swelling behavior in biodegradable adhesive hydrogels, with broad potential applications for hemostasis, wound healing, and bioelectronic interfaces.

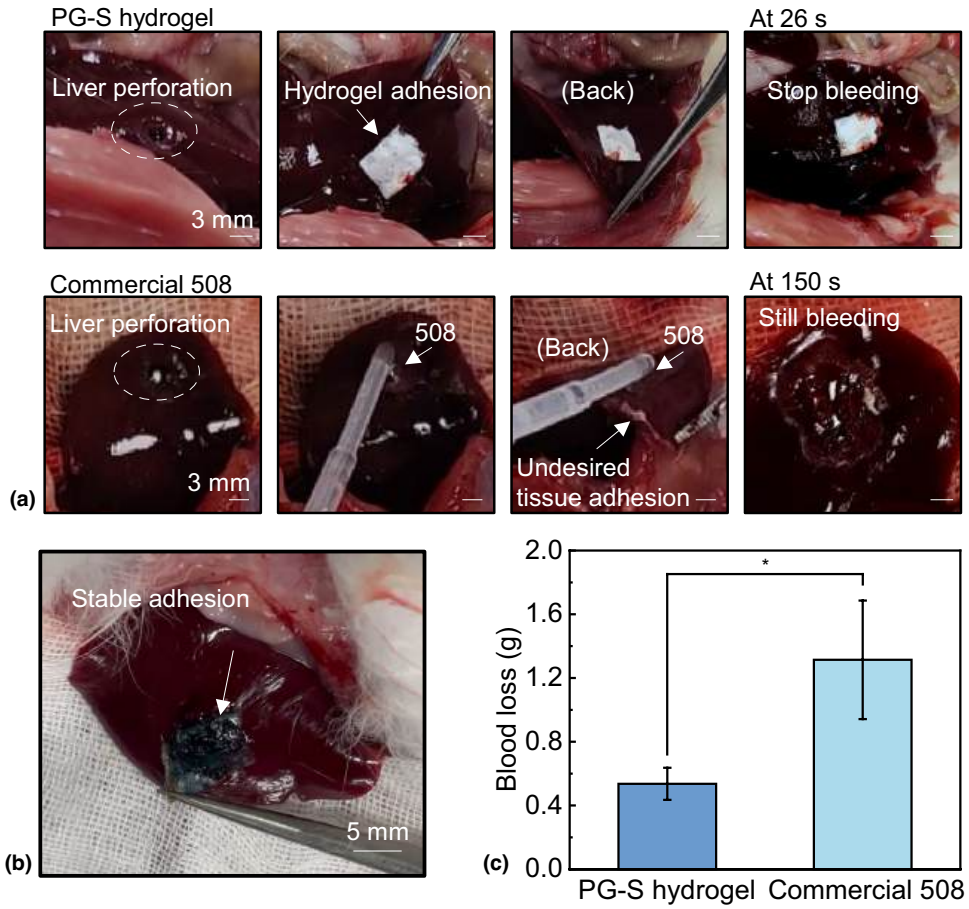

Figure 4. Hemostatic performance of the hydrogel and a commercial adhesive (508 medical glue) in a liver rupture model in SD rats. (a) Representative hemostasis process using the hydrogel and 508 tissue adhesive in models of liver perforation and rupture. (b) Stable adhesion of the hydrogel to liver tissue under tensile force after 5 min of adhesion. (c) Comparison of blood loss between the hydrogel and commercial adhesive during the hemostasis process. In (c) data are presented as mean ± standard deviation. $n = 3$ independent experiments. p-value was analyzed using one-tailed unpaired t test. ($^*p < 0.05$).

Author contributions

Conceptualization: JE.T., S.L., and L.Y.; formal analysis: JE.T., S.L., J.B., B.Y., and K.C.; writing—original draft: JE.T.; writing—review and editing: JE.T. and L.Y.; and funding: X.S. and L.Y.

Funding

The project was supported by Beijing Municipal Natural Science Foundation (Z220015 to L.Y.), Tsinghua-Toyota Joint Research Fund, the National Natural Science Foundation of China (52171239 to L.Y., T2425003 and 52272277 to X.S.), Tsinghua University Initiative Scientific Research Program (2024Z02ORD001, to X.S.).

Data availability

The data that support the findings of this study are available upon request from the corresponding author.

Declarations

Conflict of interest

On behalf of all authors, the corresponding author states that there is no conflict of interest.

References

1. M. Ghovvati et al., Rapid closure and hemostasis of ruptured soft tissues using a modified human tropoelastin-based sealant in preclinical models. Sci. Transl. Med. **17**, eadr6458 (2025). https://doi.org/10.1126/scitranslmed.adr6458
2. S. Bian et al., An injectable rapid-adhesion and anti-swelling adhesive hydrogel for hemostasis and wound sealing. Adv. Funct. Mater. **32**, 2207741 (2022). https://doi.org/10.1002/adfm.202207741
3. S. Pourshahrestani, E. Zeimaran, N.A. Kadri, N. Mutlu, A.R. Boccaccini, Polymeric hydrogel systems as emerging biomaterial platforms to enable hemostasis and wound healing. Adv. Healthc. Mater. **9**, 2000905 (2020). https://doi.org/10.1002/adhm.202000905

4. C.-C. Feng et al., A hemostatic keratin/alginate hydrogel scaffold with methylene blue mediated antimicrobial photodynamic therapy. J. Mater. Chem. B. **10**, 4878–4888 (2022). https://doi.org/10.1039/D2TB00898J
5. Y. Hong et al., A strongly adhesive hemostatic hydrogel for the repair of arterial and heart bleeds. Nat. Commun. **10**, 2060 (2019). https://doi.org/10.1038/s41467-019-10004-7
6. J. Yang et al., Injectable hemostatic hydrogel adhesive with antioxidant, antibacterial and procoagulant properties for hemorrhage wound management. J. Colloid Interface Sci. **673**, 395–410 (2024). https://doi.org/10.1016/j.jcis.2024.05.207
7. G. Muñoz Taboada, P. Dosta, E.R. Edelman, N. Artzi, Sprayable Hydrogel for Instant Sealing of Vascular Anastomosis. Adv. Mater. **34**, 2203087 (2022). https://doi.org/10.1002/adma.202203087
8. Y. Ju et al., A pro-healing and antibacterial bio-based hydrogel barrier for the prevention of intestinal anastomotic leakage. ACS Appl. Mater. Interfaces **17**, 22410–22433 (2025). https://doi.org/10.1021/acsami.5c02037
9. S.I. Kang et al., Double-layer adhesives for preventing anastomotic leakage and reducing post-surgical adhesion. Mater. Today Bio. **23**, 100806 (2023). https://doi.org/10.1016/j.mtbio.2023.100806
10. Z. Wang et al., A sprayable Janus hydrogel as an effective bioadhesive for gastrointestinal perforation repair. Adv. Funct. Mater. **34**, 2408479 (2024). https://doi.org/10.1002/adfm.202408479
11. Y. Xue et al., Trigger-detachable hydrogel adhesives for bioelectronic interfaces. Adv. Funct. Mater. **31**, 2106446 (2021). https://doi.org/10.1002/adfm.202106446
12. J. Lao et al., Intrinsically adhesive and conductive hydrogel bridging the bioelectronic-tissue interface for biopotentials recording. ACS Nano **19**, 7755–7766 (2025). https://doi.org/10.1021/acsnano.4c12823
13. Q. Zhang et al., Multi-functional adhesive hydrogel as bio-interface for wireless transient pacemaker. Biosens. Bioelectron. **263**, 116597 (2024). https://doi.org/10.1016/j.bios.2024.116597
14. K. Shen et al., A wet-adhesion and swelling-resistant hydrogel for fast hemostasis, accelerated tissue injury healing and bioelectronics. Adv. Mater. **37**, 2414092 (2025). https://doi.org/10.1002/adma.202414092
15. Q. Yang et al., Photocurable bioresorbable adhesives as functional interfaces between flexible bioelectronic devices and soft biological tissues. Nat. Mater. **20**, 1559–1570 (2021). https://doi.org/10.1038/s41563-021-01051-x
16. H. Liu et al., A highly-stretchable and adhesive hydrogel for noninvasive joint wound closure driven by hydrogen bonds. Chem. Eng. J. **452**, 139368 (2023). https://doi.org/10.1016/j.cej.2022.139368
17. P. Ma et al., Super-structured wet-adhesive hydrogel with ultralow swelling, ultrahigh burst pressure tolerance, and anti-postoperative adhesion properties for tissue adhesion. Adv. Mater. **36**, 2305400 (2024). https://doi.org/10.1002/adma.202305400
18. M. Maw et al., Sticky architecture: Encoding pressure sensitive adhesion in polymer networks. ACS Cent. Sci. **9**, 197–205 (2023). https://doi.org/10.1021/acscentsci.2c01407
19. J. Yu et al., Molecular architecture regulation for the design of instant and robust underwater adhesives. Sci. Adv. **9**, eadg4031 (2023). https://doi.org/10.1126/sciadv.adg4031
20. H. Yang et al., Reversible, ultra-strong underwater adhesive based on supramolecular interaction for instant liquid leakage sealing and robust tissue adhesion. Chem. Eng. J. **480**, 148064 (2024). https://doi.org/10.1016/j.cej.2023.148064
21. Q. Dong et al., Rapid forming, robust adhesive fungal-sourced chitosan hydrogels loaded with deferoxamine for sutureless short-gap peripheral nerve repair. Adv. Healthc. Mater. **13**, 2401412 (2024). https://doi.org/10.1002/adhm.202401412
22. X. Ma et al., Hydrogels for underwater adhesion: Adhesion mechanism, design strategies and applications. J. Mater. Chem. A **10**, 11823–11853 (2022). https://doi.org/10.1039/D2TA01960D
23. J. Wu et al., An off-the-shelf bioadhesive patch for sutureless repair of gastrointestinal defects. Sci. Transl. Med. **14**, eabh2857 (2022). https://doi.org/10.1126/scitranslmed.abh2857
24. S. Liu et al., A biodegradable, adhesive, and stretchable hydrogel and potential applications for allergic rhinitis and epistaxis. Adv. Healthc. Mater. **12**, 2302059 (2023). https://doi.org/10.1002/adhm.202302059
25. Y. Qin et al., In situ self-assembly of nanoparticles into waxberry-like starch microspheres enhanced the mechanical strength, fatigue resistance, and adhesiveness of hydrogels. ACS Appl. Mater. Interfaces **12**, 46609–46620 (2020). https://doi.org/10.1021/acsami.0c10327
26. N. Sato, Y. Aoyama, J. Yamanaka, A. Toyotama, T. Okuzono, Particle adsorption on hydrogel surfaces in aqueous media due to van der Waals attraction. Sci. Rep. **7**, 6099 (2017). https://doi.org/10.1038/s41598-017-06257-1
27. R. Ahmed et al., Genipin, a natural blue colorant precursor: Source, extraction, properties, and applications. Food Chem. **434**, 137498 (2024). https://doi.org/10.1016/j.foodchem.2023.137498
28. Z. Zhou, J. Lei, Z. Liu, Effect of water content on physical adhesion of polyacrylamide hydrogels. Polymer **246**, 124730 (2022). https://doi.org/10.1016/j.polymer.2022.124730
29. S. Rose, A. Dizeux, T. Narita, D. Hourdet, A. Marcellan, Time dependence of dissipative and recovery processes in nanohybrid hydrogels. Macromolecules **46**, 4095–4104 (2013). https://doi.org/10.1021/ma400447j
30. X. Hu, M. Vatankhah-Varnoosfaderani, J. Zhou, Q. Li, S.S. Sheiko, Weak hydrogen bonding enables hard, strong, tough, and elastic hydrogels. Adv. Mater. **27**, 6899–6905 (2015). https://doi.org/10.1002/adma.201503724
31. J. Yang, C.-R. Han, X.-M. Zhang, F. Xu, R.-C. Sun, Cellulose nanocrystals mechanical reinforcement in composite hydrogels with multiple cross-links: Correlations between dissipation properties and deformation mechanisms. Macromolecules **47**, 4077–4086 (2014). https://doi.org/10.1021/ma500729q